Dalton Transactions

Cite this: *Dalton Trans.*, 2011, **40**, 5720

www.rsc.org/dalton

PAPER

Entropically driven self-assembly of a strained hexanuclear indium metal–organic macrocycle and its behavior in solution†

Minhak Oh,[a] Xinfang Liu,[a,b] Mira Park,[b] Dongwook Kim,[a] Dohyun Moon*[c] and Myoung Soo Lah*[a]

Received 9th February 2011, Accepted 18th March 2011
DOI: 10.1039/c1dt10220f

The self-assembly of a polyprotic pentadentate ligand, *N*-cyclopentanoylaminobenzoylhydrazide (H_4L^4), and an In(III) nitrate hydrate in methanol led to a strained hexanuclear indium metal–organic macrocycle (In–MOM), $[In(III)_6(H_2L^4)_6(NO_3)_x(solvent)_{6-x}](NO_3)_{6-x}$ (where, the solvent is either methanol or a water molecule and x is the number of the nitrate anions ligated). The ligand in the doubly deprotonated state serves as an unsymmetric linear ditopic donor and the alternating indium ions in two different chelation modes serve as two different bent ditopic metal acceptors, which led to a D_3-symmetric hexanuclear In–MOM. Although the hexanuclear In–MOM is enthalpically unfavorable because of the ring strain, the combination of the soft coordination characteristic of the indium ion and the slight ligand deformation from the conjugated planar conformation allows the formation of the entropically favored hexanuclear In–MOM rather than the enthalpically favored octanuclear In–MOM. While the hexanuclear In–MOM is stable in acetonitrile, it partially dissociates into its components in dimethylsulfoxide, and then slowly reaches a new equilibrium state with several different indium species yet to be identified in addition to the free ligand.

Introduction

Metal–organic systems (MOSs), such as metal–organic frameworks (MOFs)[1] and metal–organic polyhedra (MOP),[2] have received much attention from researchers over two decades because of their interesting properties and potential applications in diverse areas. However, the prediction or design of the resulting systems from the building components is still challenging. A small change in building blocks or synthetic conditions often leads to a quite unexpected result. A metal–organic macrocycle (MOM)[3] could be used as a simple model system to understand the self-assembly phenomenon in complicated MOSs. The self-assembly of ditopic donor and ditopic acceptor components might generate either an infinite 1-D chain or a finite MOM, where the ditopic building components alternate in the system. For the construction of a finite MOM, at least one building component, either the ditopic metal ion as an acceptor component or the dipotic organic ligand as a donor component must be a bent component; otherwise, an infinite 1-D chain will be generated.

We have reported the preparation and characterization of several MOMs using potential pentadentate ligands, *N*-acylsalicylhydrazides, as a ditopic donor component.[4] Combining the ligand with a metal ion with +3 oxidation state preferring octahedral coordination geometry led to a cyclic repetition of the metal component and the ligand to form an MOM. In the MOM, the pentadentate ligand serves as an unsymmetric linear ditopic donor that interconnects two metal ions *via* a five- and six-membered *mer*-tridentate chelation mode around one metal ion and a five-membered bidentate chelation mode around the other metal ion (Scheme 1).

The metal ion in the *mer*-tridentate chelation and bidentate chelation modes from the two ligands serves as a bent ditopic acceptor (Scheme 2(a)). A small change in the *N*-acylsalicylhydrazide, such as the substitution of an amino group for the hydroxyl group of the *N*-acylsalicylhydrazide, produced a subtle difference in the coordination behavior of the new amino-substituted ligand, *N*-acylaminobenzoylhydrazide ligand, in the MOM depending on the metal ion used.[5,6] The reaction of *N*-acetylaminobenzoylhydrazide (H_4L^1) with manganese ions led to the S_6-symmetric hexanuclear Mn–MOM, $[Mn(III)_6(HL^1)_6(solvent)_6]$,[5] which is isostructural to the hexanuclear Mn–MOM, $[Mn(III)_6(L^2)_6(solvent)_6]$, obtained when

[a]*Interdisciplinary School of Green Energy, Ulsan National Institute of Science & Technology, Ulsan, 689-798, Korea. E-mail: mslah@unist.ac.kr; Fax: 82 52 217 2019; Tel: 82 52 217 2931*

[b]*Department of Chemistry and Applied Chemistry, Hanyang University, Ansan, Kyunggi-do, 426-791, Korea*

[c]*Pohang Accelerator Laboratory, Pohang, Kyungbook, 790-784, Korea. E-mail: dmoon@postech.ac.kr; Tel: 82 54 279 1547*

† Electronic supplementary information (ESI) available: ^{1}H NMR spectrum and ^{13}C NMR spectrum of H_4L^4, ^{1}H NMR spectra of the two different crystalline forms, **1** and **2**, in d_6-dmso with expansion of the 0.5–3.2 ppm range, time dependent ^{1}H NMR spectra of **2** in d_6-dmso with expansion of the 0.5–3.2 ppm range, IR spectra of the **1** + **2** mixture and **2**, ORTEP diagrams of **1** and **2** with full numbering, CPK diagram of **2**, the conformations of the ligand in **1** and the Ga–MOM, hydrogen bond table for **1**, the bond distance and angle table around the metal ions for **1** and Ga–MOM, and the details of the crystal structure determinations, X-ray crystallographic files (CIF) of **1** and **2**. CCDC reference numbers 813982 and 813983. For ESI and crystallographic data in CIF or other electronic format see DOI: 10.1039/c1dt10220f

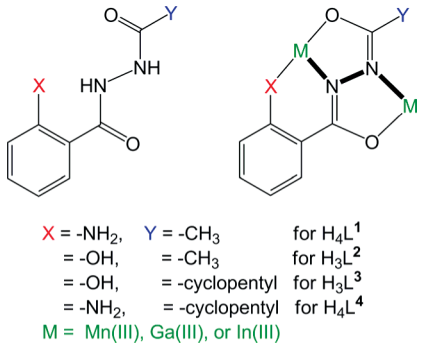

Scheme 1 Ligands and their asymmetric bridging mode.

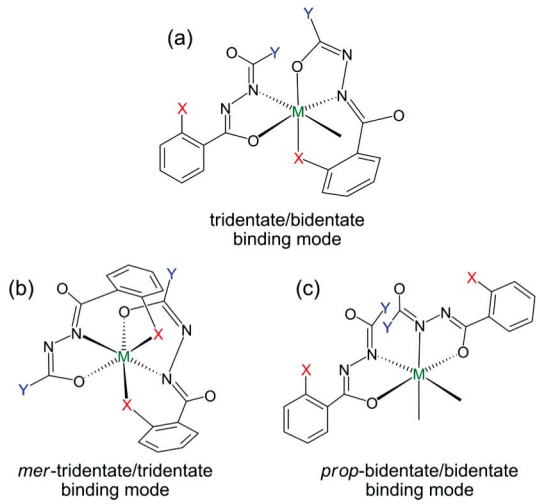

Scheme 2 Binding modes of the ligands around the metal center.

N-acetylsalicylhydrazide (H_3L^2) is used as the ligand.[4g] While the reaction of *N*-cyclopentanoylsalicylhydrazide (H_3L^3) with manganese ions leads to the S_{10}-symmetric decanuclear Mn–MOM, $[Mn(III)_{10}(L^3)_{10}(solvent)_{10}]$,[4f] a similar reaction of the same ligand with gallium ions leads to an S_8-symmetric octanuclear Ga–MOM, $[Ga(III)_8(L^3)_8(solvent)_8]$, which has the same cyclic repetition of the metal ion (Scheme 3) and the ligand, but has reduced the nuclearity from ten to eight metal ions in the corresponding MOMs.[6] However, a similar reaction using the amino-substituted ligand, *N*-cyclopentanoylaminobenzoylhydrazide (H_4L^4), with gallium ions resulted in a D_4-symmetric octanuclear Ga–MOM, $[Ga(III)_8(H_2L^4)_8(solvent)_8](NO_3)_8$, with different ligand connectivity compared with the connectivity in the S_n-symmetric MOMs prepared using *N*-acylsalicylhydrazides (Scheme 3).[6]

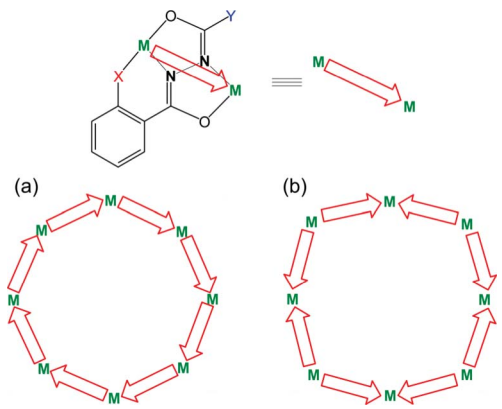

Scheme 3 Two different ligand connectivities of the asymmetric ditopic ligand in an MOM.

Even though both ligands serve as the same pentadentate ditopic bridging ligands in the MOMs, their protonation states and the charges are not the same. When the triply deprotonated trianionic ligands with a single amino hydrogen atom are used as bridging ligands between the metal ions, the ligands are involved in a *mer*-tridentate/bidentate binding mode around a metal ion and the cyclic repetition of the metal ions generates an MOM with S_n-symmetry.[4,5] When the doubly deprotonated dianionic ligand with two amino hydrogen atoms is used as a bridging ligand between the metal ions, the alternative *mer*-tridentate/tridentate binding mode and *prop*-bidentate/bidentate binding mode at the metal ions (Schemes 2(b) and 2(c)) lead to a D_4-symmetric octanuclear MOM with a different ligand connectivity.[6]

We report herein the preparation and characterization of a new In–MOM using the amino-substituted potential pentadentate ligand, H_4L^4, to see the effects of the metal ion on the protonation state of the ligand, the connectivity between the metal ions, the coordination geometries around the metal ions, the nuclearity (or ring size) of the MOM, and the symmetry of the MOM.

Experimental

Materials and instrumentation

Reagents and solvents for syntheses were purchased from commercial sources and used as received. Elemental analyses (C, H, and N) were performed using a Thermo Scientific Flash 2000 elemental analyzer. Infrared spectra were recorded in the range 4000–600 cm^{-1} on a Varian 670 FT-IR spectrophotometer. ^1H and ^{13}C NMR spectra were obtained using a Varian-600 spectrometer. Electrospray ionization (ESI) mass spectra were recorded using a Bruker HCT Basic System. H_4L^4 was prepared according to the literature procedure.[6] ^1H NMR spectrum (dmso-d_6, δ ppm) of H_4L^4: 9.91 (s, 1H), 9.67 (s, 1H), 7.52 (d, 1H), 7.16 (t, 1H), 6.71 (d, 1H), 6.50 (t, 1H), 6.38 (s, 2H), 2.67 (q, 1H), 1.79 (m, 2H), 1.62–1.72 (m, 4H), 1.53 (m, 2H). ^{13}C NMR spectrum (dmso-d_6, δ ppm) of H_4L^4: 174.91, 167.89, 149.71, 132.04, 128.01, 116.23, 114.44, 112.55, 42.05, 29.83, 25.64 (Fig. S1†).

Preparation of hexanuclear In–MOM

Method A. A 24.2 mg (0.098 mmol) sample of H_4L^4 was dissolved in 15 mL anhydrous MeOH in a 20 mL vial and a 40.9 mg (0.105 mmol) sample of $In(NO_3)_3{\cdot}5H_2O$ was slowly added. The solution was left to stand for 5 d at 0 °C in the refrigerator and gave two different morphologies of colorless crystals, block-shaped crystal **1** and needle-shaped crystal **2**. The crystalline mixture in an approximately 7 : 3 ratio of the two forms (based on a visual inspection) was filtered off and air-dried before elemental analysis. Yield 7.8 mg, 29%. Analysis data for the crystalline mixture. Elemental analysis calculated for $In_6(H_2L^4)_6(NO_3)_6(H_2O)_{16}$ ($C_{78}H_{122}N_{24}O_{46}In_6$, fw = 2820.88): C 33.21, H 4.36, N 11.92%; found: C 32.98, H 4.01, N 12.05%. IR (KBr pellet, cm^{-1}): 3251, 2958, 2871, 1614, 1595, 1510, 1497, 1472, 1449, 1417, 1386, 1332,

Table 1 Crystal data and structure refinements for **1** and **2**

	1	**2**
Empirical formula	$In_6C_{85}H_{121}N_{24}O_{40.50}$	$In_9C_{117}H_{153}N_{36}O_{54}$
Formula weight	2815.98	3961.13
Temperature/K	100(2)	100(2)
Wavelength/Å	0.70000	0.75000
Crystal system	Orthorhombic	Tetragonal
Space group	*Iba*2	*P*-4*c*2
Unit cell dimensions/Å	$a = 22.955(5)$	$a = 29.234(4)$
	$b = 47.028(9)$	$b = 29.234(4)$
	$c = 20.745(4)$	$c = 39.139(8)$
Volume/Å^3	22395(8)	33449(9)
Z	8	8
Absorption coefficient/mm^{-1}	1.308	1.305
Crystal size/mm^3	$0.13 \times 0.13 \times 0.05$	$0.50 \times 0.10 \times 0.08$
Reflections collected	59544	15840
Independent reflections	15841 [R(int) = 0.0890]	25059 [R(int) = 0.1151]
Max. and min. transmission	0.9375 and 0.8483	0.9028 and 0.5614
Goodness-of-fit on F^2	0.957	1.030
Final R indices [$I > 2\sigma(I)$]	$R_1 = 0.0554$, $wR_2 = 0.1297$	$R_1 = 0.0984$, $wR_2 = 0.2833$
R indices (all data)	$R_1 = 0.0841$, $wR_2 = 0.1425$	$R_1 = 0.1263$, $wR_2 = 0.3030$
Absolute structure parameter	0.07(3)	0.50(4)
Largest diff. peak and hole, e Å^{-3}	0.780 and –0.981	1.372 and –0.991

1312, 1297, 1163, 1146, 1097(sh), 1076, 1054, 916, 871, 816, 781, 755, 701, 676, 667, 646, 637, 623 (Fig. S2†).

Method B. A 24.2 mg (0.098 mmol) sample of H_4L^4 was dissolved in 15 mL MeOH–H_2O mixed solvent (15 : 1 ratio) in a 20 mL vial and a 40.9 mg (0.105 mmol) sample of $In(NO_3)_3 \cdot 5H_2O$ was slowly added. The solution was left to stand for 5 d at room temperature and gave needle-shaped crystal **2** as the only crystalline product. The crystals were filtered off and air-dried before elemental analysis. Yield 7.5 mg, 28%. Elemental analysis calculated for $In_6(H_2L^4)_6(NO_3)_6(H_2O)_{13}$ ($C_{78}H_{116}N_{24}O_{43}In_6$, fw = 2766.83): C 33.86, H 4.23, N 12.15%; found: C 33.95, H 4.20, N 12.03%. IR (cm^{-1}): 3251, 2958, 2871, 1614, 1595, 1510, 1497, 1472, 1449, 1415, 1386, 1337, 1312(sh), 1297, 1163, 1146, 1092(sh), 1075, 1054, 916, 871, 816, 782, 755, 701, 686, 667, 646, 632, 613 (Fig. S2†). ^{1}H NMR spectrum of **2** (dmso-d_6, δ ppm): 7.61 (d, 1H), 7.48 (t, 1H), 7.30 (t, 1H), 7.23 (d, 1H), 6.97 (s, 2H), 2.67 (m, 1H), 1.78 (m, 1H), 1.41 (m, 1H), 1.31 (m, 1H) 1.09 (m, 1H), 0.92–1.02 (m, 3H), 0.76 (m, 1H).

Crystal structure determination

Crystals of **1** and **2** were coated with paratone oil and the diffraction data were measured at 100 K with synchrotron radiation on a 6B MX-I ADSC Quantum-210 detector with a silicon (111) double-crystal monochromator at the Pohang Accelerator Laboratory, Korea. The ADSC Quantum-210 ADX program (Ver. 1.92)[7] was used for data collection, and the HKL2000 (Ver. 0.98.699) program[8] was used for cell refinement, reduction, and absorption correction. The structures were solved by direct methods and refined by full-matrix least-squares calculations with the SHELXTL-PLUS software package.[9]

$[In_6(H_2L^4)_6(NO_3)(MeOH)_4(H_2O)](NO_3)_5$, 1. A hexanuclear In–MOM with one nitrate anion and five solvent molecules (four methanol molecules and one water molecule) ligated to three alternating metal ions, five additional nitrate counter anions, and at least six structural solvent sites (four methanol molecules and two statistically disordered water molecules) were identified as an asymmetric unit.

$[In_6(H_2L^4)_6(H_2O)_6](NO_3)_6$, 2. One and a half hexanuclear In–MOMs with a half on a crystallographic two-fold axis were identified as an asymmetric unit. All of the potential ligated solvent sites in the MOMs are occupied by water molecules (the data quality of the structure does not provide unambiguous identities of the ligated solvent sites as some of them could be either partially identified methanol molecules or nitrate anions). Two additional water sites were identified; both of them were in the center of the hexanuclear In–MOM. No nitrate anions were identified in the difference Fourier map. Further structure refinement was performed after modification of the data for the lattice solvent molecules and the unidentified disordered nitrate anions (10101 Å^3, 30.4% of the crystal volume) using the *SQUEEZE* routine of the PLATON software package (Ver. 130605).[10]

A summary of the crystal and intensity data is given in Table 1.

The details of the crystal structure determination is provided in the supplementary information. CCDC 813982 (for **1**) and 813983 (for **2**) contain the supplementary crystallographic data for this paper.

Results and discussion

While ligand H_4L^4 is self-assembled with In(III) nitrate pentahydrate in a 1 : 1 ratio in anhydrous methanol, block-shaped colorless crystals, **1**, and needle-shaped colorless crystals, **2**, were simultaneously obtained in an approximately 7 : 3 ratio, the similar reaction in a methanol–water mixed solvent (15 : 1 ratio) led only to needle-shaped colorless crystals, **2**. The structure analysis of a block-shaped crystal revealed **1** to be an 18-membered hexanuclear In–MOM, $[In(III)_6(H_2L^4)_6(NO_3)(solvent)_5](NO_3)_5$ (where, $[H_2L^4]^{2-}$ is in a doubly deprotonated state and the solvent is either methanol or a water molecule) (Fig. 1 and S3†). Although the hydrogen atom positions of the amino groups were generated assuming the amino

Table 2 Intermetal distances and angles (Å and °) in **1**

M···M	*d*(M···M)	M···M···M	<M···M···M	M···M···M	<M···M···M
In1···In2	5.1878(9)	In6···In1···In2	132.393(8)		
In2···In3	5.1292(10)			In1···In2···In3	100.985(6)
In3···In4	5.1307(7)	In2···In3···In4	142.131(6)		
In4···In5	5.1131(7)			In3···In4···In5	103.052(7)
In5···In6	5.1717(10)	In4···In5···In6	130.940(6)		
In6···In1	5.1480(9)			In5···In6···In1	110.255(6)
avg.	**5.15(3)**	**avg.**	**135(6)**[a]	**avg.**	**105(5)**[b]

[a] The average <M···M···M angle around the *mer*-tridentate/tridentate binding site. [b] The average <M···M···M angle around the *prop*-bidentate/bidentate binding site.

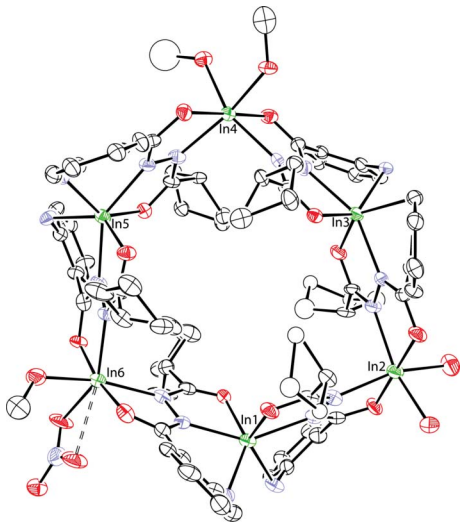

Fig. 1 An ORTEP diagram of **1** with 20% of thermal ellipsoid probability displacement. For the sake of clarity all hydrogen atoms as well as counter ions have been omitted.

nitrogen atoms to be in the sp^3-hybridization form, the hydrogen-bonding patterns (Table S1†) and the charge balance based on the number of nitrate anions in the single-crystal structure suggest that all of the ligands are in a doubly deprotonated dianionic state. As in the other MOMs, the pentadentate ligand serves as an unsymmetric ditopic bridging ligand between two indium ions, *via* a *mer*-tridentate chelation mode using one side of the bridging domain to a metal ion and *via* a bidentate chelation mode using the other side of the bridging domain to the other metal ion.

As in the D_4-symmetric octanuclear Ga–MOM, $[Ga(III)_8(H_2L^4)_8(solvent)_8](NO_3)_8$,[6] two different types of coordination geometry of the indium ions, one in a *mer*-tridentate/tridentate chelation mode and the other in a *prop*-bidentate/bidentate chelation mode, were observed in **1**. An octahedral In(III) ion with *mer*-tridentate/tridentate chelation mode in the MOM is in the *C* (counterclockwise) chiral configuration based on the rotational sense of the two *mer*-tridentate chelating domains (Fig. 2a). The other In(III) ion with *prop*-bidentate/bidentate chelation mode is in the Δ chiral configuration based on the rotational sense of the two bidentate chelating domains in a propeller configuration (Fig. 2b).

A cyclic repetition of the two alternating chiral metal ions leads to the pseudo-D_3-symmetric hexanuclear In–MOM, where the metal ions are in the $\cdots(M_CM_\Delta)(M_CM_\Delta)\cdots$ chiral sequence. The

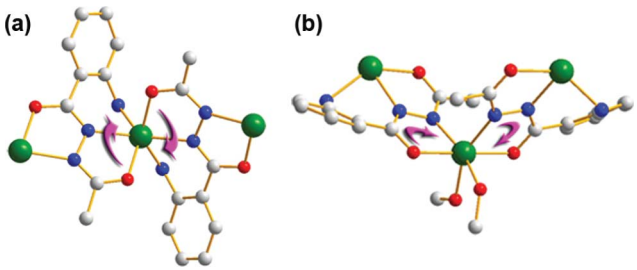

Fig. 2 Two different coordination geometries of the indium ions in In–MOM, (a) one in a *mer*-tridentate/tridentate chelation mode in the *C* chiral configuration and (b) the other in a *prop*-bidentate/bidentate chelation mode in the Δ chiral configuration. Color codes: indium (green), oxygen (red), nitrogen (blue), and carbon (gray).

nearest inter-metal distances (In···In distances) in the In–MOM (Table 2) are in the expected range, 5.1131(7)–5.1878(9) Å, with an average value of about 5.15(3) Å. The average distance is similar to those in other MOMs having a similar diaza-bridged M–N–N–M connectivity.[4] However, the In···In···In angles in **1** are quite different from those in the S_n-symmetric MOMs, where only one type of metal ion of the *mer*-tridentate/bidentate binding mode exists and, as a consequence, there is only one type of M···M···M angle, which is strongly correlated with the size of the macrocycle and the extent of the ring puckering.[4,5] As in the D_4-symmetric MOM with two different alternating chiral metal ions,[6] there are two different types of In···In···In angles in **1** (Table 2). The average In···In···In angle with the central metal ion with *prop*-bidentate/bidentate coordination geometry is 105(5)°, which is slightly smaller than the corresponding value observed in the D_4-symmetric octanuclear Ga–MOM, 111(2)°. While the In···In···In angle with the central metal ion in an ideal *mer*-tridentate/tridentate coordination geometry with no other structural restraints will be 180°, the average value of the corresponding angles in **1** is 135(6)°, which is even smaller than the value observed in the similar but D_4-symmetric octanuclear MOM, 158(2)°. The distortion toward the smaller In···In···In angle is the result of the larger ring strain imposed by the smaller macrocyclic ring size in the D_3-symmetric hexanuclear In–MOM, **1**, than that in the D_4-symmetric octanuclear Ga–MOM. The effect of the ring strain in the smaller MOM, D_3-symmetric hexanuclear In–MOM, is also reflected in the coordination geometry of the In(III) ion and in the conformation of the ligand. The coordination geometry of the octahedral In(III) ion with the *mer*-tridentate/tridentate chelation mode is more distorted from the ideal octahedral geometry than the coordination geometry of

the corresponding metal ion of the Ga–MOM (Table S2†). The softer coordination characteristic of the In(III) ion than that of the Ga(III) ion,‡ which results from the larger metal ion size of the In(III) ion compared with that of the Ga(III) ion and the consequent larger metal–ligand distance (Table S3†), allows the larger distortion of the coordination geometry of the In(III) ion from the ideal octahedral geometry to release the ring strain in the smaller ring system. The ring strain in the hexanuclear MOM could also be released through the conformation change of the ligand. The dihedral angle between the two planar residues in the ligand (one plane consists of the aminophenyl group and the other plane consists of the conjugated bridging domain), which is directly related to the overall conformation of the ligand, is more deformed in the In–MOM from the ideal conjugated planar conformation of the ligand than that in the Ga–MOM toward a less planar conformation (Fig. S4†). The average dihedral angle between the two planar residues of the ligand in the In–MOM (34(3)°) is slightly larger than that observed in the Ga–MOM (27(3)°).

The structural analysis of a needle-shaped crystal revealed that **2** had the same 18-membered hexanuclear In–MOM structure as that of **1**. However, poor crystallographic data quality limited the unambiguous identification of the ligated monodentate species and the protonation state of the ligands in **2**, $[In(III)_6(H_2L^4)_6(NO_3)_x(solvent)_{6-x}](NO_3)_{6-x}$ (where, $[H_2L^4]^{2-}$ is in a doubly deprotonated state, the solvent is either methanol or a water molecule, and x is the number of the nitrate anions ligated) (Fig. S5†). The ligand in **2** was assumed to be in a doubly deprotonated state, $[H_2L^4]^{2-}$, the same as the protonation state of the ligand in **1**.

The formation of an In–MOM with smaller ring size is enthalpically unfavorable because of the increased ring strain in the system. However, the combination of the larger geometry tolerance of the indium ion having a soft coordination characteristic toward distorted coordination geometry and a small enthalpy cost for the ligand deformation from the conjugated planar conformation allows the formation of the D_3-symmetric hexanuclear 18-membered In–MOM. The real driving force for the formation of the In–MOM with an increased ring strain in the reduced macrocyclic ring size is the entropy factor that comes from the smaller number of components in the macrocyclic system. A similar behavior has also been reported in the trinuclear Pt–MOMs,[11] where the self-assembly of a rigid linear ditopic donor, pyrazine, and a bent ditopic acceptor, *cis*-blocked Pt(II) ion, preferring 90° angle led to a triangular strained-cyclic arrangement rather than a square relaxed-cyclic arrangement because of the entropy factor.

Because the species in the solid state is not always consistent with that observed in the solution state, the identity of the In–MOM in solution was investigated using ^{1}H NMR spectroscopy and ESI mass spectrometry. The solution behavior of the two different crystalline forms based on their ^{1}H NMR spectra in dimethylsulfoxide (dmso) are similar to each other (Fig. 3 and S6†), hence only the ^{1}H NMR spectra of **2** will be discussed.

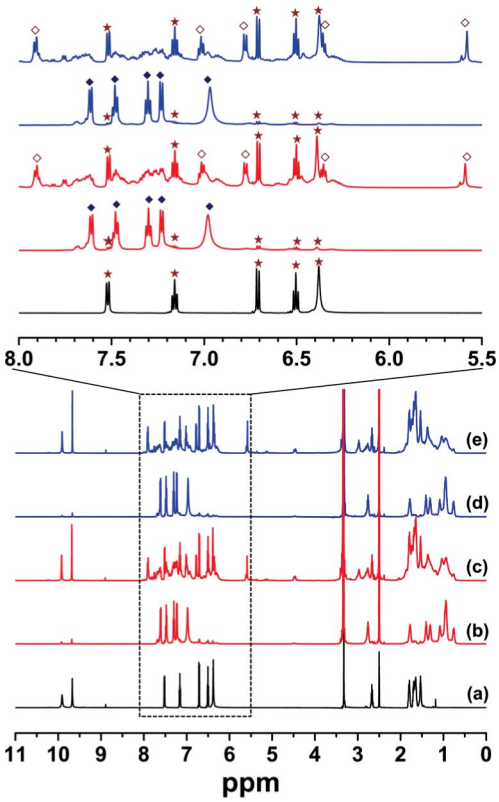

Fig. 3 ^{1}H NMR spectra of two different crystalline forms, **1** and **2**, in d_6-dmso with an expansion of the 5.5–8.0 ppm range. ^{1}H NMR spectra of (a) H_4L^4, (b) **1** taken within 5 min after the preparation, (c) **1** taken at its equilibrium state, (d) **2** taken within 5 min after the preparation, and (e) **2** taken at its equilibrium state. ★ is for the free ligand, ◆ is for **2**, and ◇ is for the new species, **3**, in the equilibrium state.

The initial ^{1}H NMR spectrum of **2** was taken within 5 min after the preparation of the sample in dmso solvent. The spectrum shows five peaks slightly shifted downfield from those of the free ligand in the aromatic region (5.5–8.0 ppm) for the aromatic and amino hydrogen atoms (Fig. 3). Nine broad peaks around the 0.5–3.0 ppm region are for the hydrogen atoms of the cyclopentyl residue in an asymmetric environment, which contrasts with the five peaks around the same region for the hydrogen atoms of the cyclopentyl residue of the free ligand in a symmetric environment (Fig. 3 and S6†). The downfield shift of the aromatic peaks indicates that the ligand is ligated to the metal ion, and the asymmetric environment of the cyclopentyl residue implies that the rotation of the cyclopentyl group is restricted in the solution species, as is that of the cyclopentyl groups of the hexanuclear In–MOM in the crystal structure (Fig. S7†). The combination of the coordination of the ligand to the metal ion and the restricted rotational degrees of freedom of the cyclopentyl residue strongly suggests that the hexanuclear In–MOM structure observed in the solid state is maintained in dmso solution. However, a careful examination of the ^{1}H NMR spectrum also shows the presence of proton peaks corresponding to those of the free ligand. Some hexanuclear In–MOM species have dissociated into their building components in dmso solution. The hexanuclear In–MOM slowly

‡ Because both In(III) and Ga(III) ions belong to Group 13 in Periodic Table, they do not have any crystal field stabilization energies and do have little preference for some specific coordination geometries. The coordination geometries of In(III) and Ga(III) ions are mainly determined by electronic and steric effects of the ligated ligands. The larger In(III) ion is more polarizable and has lesser coordination preference for specific geometry than the smaller Ga(III) ion.

dissociates into the free ligand, the amount of free ligand increases, and then a new species, **3**, appears after the free ligand, the solution reaching an equilibrium state with three major species, **2**, H_4L^4, and **3**, in an approximately 1 : 2 : 2 ratio within about 9 h (Fig. 4 and S8†).

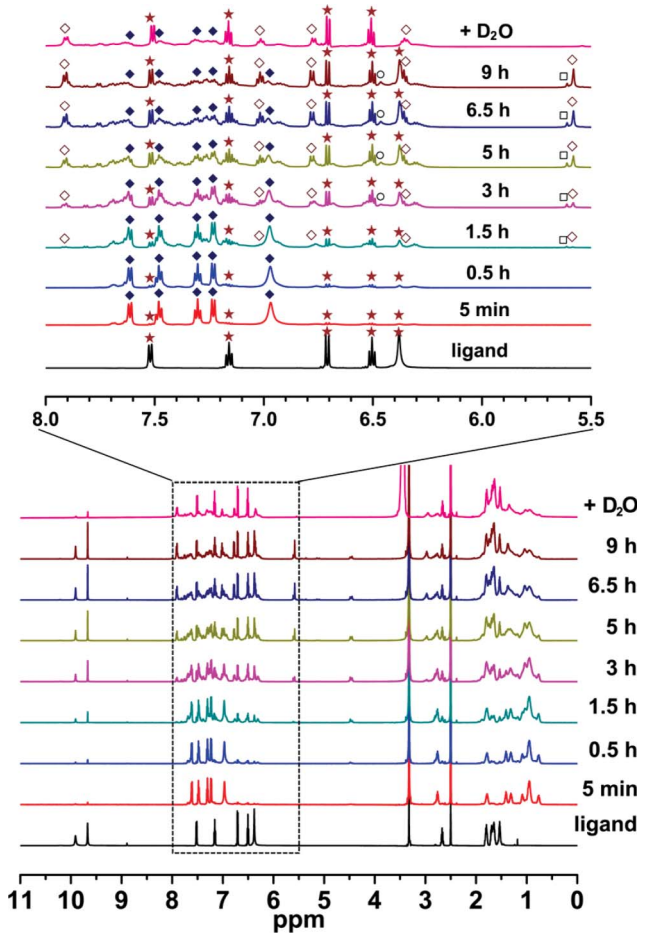

Fig. 4 The time dependent ^{1}H NMR spectra of **2** in d_6-dmso with an expansion of the 5.5–8.0 ppm range. The solution reaches the equilibrium state within 9 h and is stable for more than a month. At least five different species could be identified based on the deuterium exchange experiment for the replaceable amino protons. While all of the proton peaks of the three major species in the equilibrium state (H_4L^4 (★); **2** (◆); **3** (◇)) can be assigned, only the peaks for the amino protons of the remaining two minor species (○; □) are assigned because of the lower intensities and the overlap with other peaks.

The presence of two additional minor species has been confirmed from the D_2O-added ^{1}H NMR spectrum in its equilibrium state. Five peaks corresponding to the amino protons from five different species were identified. A careful examination of the spectrum indicates a decrease in the relative intensity of the peaks corresponding to the new species, **3**, compared with that of the free ligand. The solution reaches a new equilibrium within a week with the reduced **3**/H_4L^4 ratio, ~0.2, compared with the ratio of ~1 in pure dmso solution. This fact suggests that **3** has lower stability in presence of water than it has in pure dmso. The relative intensity of the amino protons compared with the intensities of the other aromatic protons of the ligand in **3** in the equilibrium state suggests that all or at least most ligands are in a triply deprotonated state, $[HL^4]^{3-}$, with a single amino proton, rather than a doubly deprotonated state, $[H_2L^4]^{2-}$, with two amino protons.

The hexanuclear In–MOM, **2**, is stable in acetonitrile–dmso mixed solvent (20 : 1 ratio) unlike the case in pure dmso solvent. The ^{1}H NMR spectrum of **2** taken within 5 min after the preparation of the sample in the mixed solvent shows four peaks slightly shifted downfield from those of the free ligand in the aromatic region (5.5–8.0 ppm), a broad peak around 7.2 ppm overlaying to the aromatic proton peaks for the amino protons, and nine broad peaks around the 0.5–3.0 ppm region for the cyclopentyl residue in an asymmetric environment (Fig. 5). The presence of the broad peak for the amino residue was further supported by the replacement of the proton by deuterium using a D_2O-addition experiment. The ^{1}H NMR spectrum in the mixed solvent does not indicate any hint of decay of **2** even after 1 d. While **2** in pure dmso reaches an equilibrium with at least four other species, including the free ligand and **3** within 9 h, **2** is stable at least for 1 d in the acetonitrile–dmso mixed solvent.

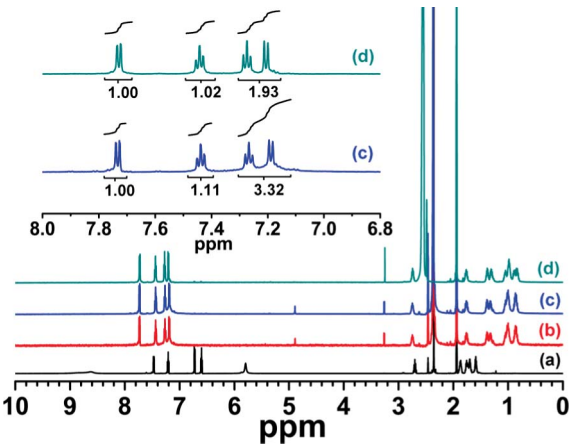

Fig. 5 The time dependent ^{1}H NMR spectra of **2** in CD_3CN–d_6-dmso (20 : 1 ratio) mixed solvent with an expansion of the 6.8–8.0 ppm range. (a) H_4L^4, (b) **2** taken within 5 min after the preparation of the solution, (c) **2** taken after 1 d, and (d) **2** taken after the addition of D_2O to solution (c). The difference in the integration values around 7.2 ppm in the spectra of (c) and (d) indicates the presence of a replaceable broad peak for the amino group of the ligand.

The ESI mass spectra of **2** in the acetonitrile–dmso mixed solvent also support the stability of **2** in the mixed solvent (Fig. 6). There is no difference between the ESI mass spectrum of **2** taken immediately after the preparation of the solution and that taken after 1 d. The $\{[In_6(H_2L)_5(HL)](NO_3)_3\}^{2+}$ ion has been observed at m/z = 1172.4 as a base peak (Fig. 6a). The observed isotope distribution pattern of the peak matches well with the calculated pattern based on the given formula (Fig. 6b).

The addition of a drop of deuterated water immediately replaces all of the potential replaceable protons with deuterons. The amino protons of the hexanuclear In–MOM, $\{[In_6(H_2L)_5(HL)](NO_3)_3\}^{2+}$, were replaced by the deuterons to form the deuterated species, $\{[In_6(D_2L)_5(DL)](NO_3)_3\}^{2+}$ ion (Fig. 7).

In the mass spectrum of the deuterated species, the peak at m/z = 1172.6 disappears and the new peak at m/z = 1177.8 appears. The increase of about ~5.2 in the m/z value in the deuterated species supports the presence of 10 to 11 replaceable amino protons. The match between the observed and simulated mass patterns

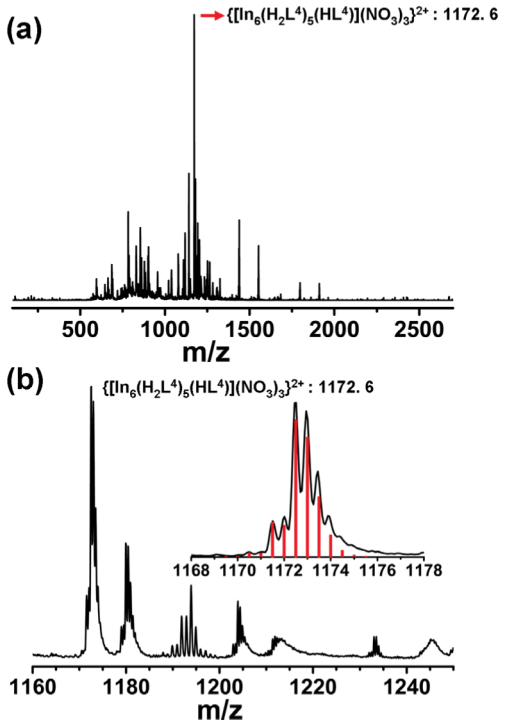

Fig. 6 The ESI mass spectrum of **2** in CD_3CN–d_6-dmso (20 : 1 ratio) mixed solvent. (a) The mass spectrum for the m/z range up to 2700 with a base peak at 1172.6 for the $\{[In_6(H_2L^4)_5(HL^4)](NO_3)_3\}^{2+}$ ion. (b) The expanded mass spectrum with an inset showing the match between the observed pattern (black solid line) and the simulated pattern (red bars) for the $\{[In_6(H_2L^4)_5(HL^4)](NO_3)_3\}^{2+}$ ion.

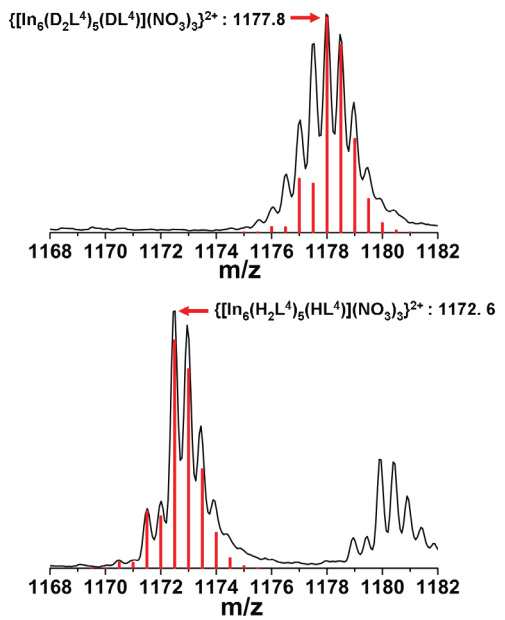

Fig. 7 The expanded mass spectra of **2** in CH_3CN–dmso (20 : 1 ratio) mixed solvent around the base peak. (a) Before and (b) after the addition of D_2O to the solution.

and the increased m/z value in the deuterated sample support the contention that one of the ligands is probably in a triply deprotonated state while the remaining five ligands are in a doubly deprotonated state.

To get mass information on **3**, **2** was dissolved in dmso and left to stand for 1 d to achieve an equilibrium state, and then the solution was diluted using acetonitrile just before the experiment. Although the ^{1}H NMR spectrum of **2** pre-matured in pure dmso and then diluted using acetonitrile in ~20 : 1 acetonitrile : dmso ratio just before the experiment was measured within 5 min, the spectrum is basically the same as that of the sample prepared using a ~20 : 1 acetonitrile : dmso ratio mixed solvent, which indicates that the reverse equilibrium process from the mixture solution of at least five different species in pure dmso to pure **2** in ~20 : 1 acetonitrile : dmso ratio mixed solvent occurs within a few minutes.

Conclusions

We have prepared an 18-membered hexanuclear In–MOM using a potential pentadentate ligand, H_4L^4, as an unsymmetric linear ditopic donor and In(III) ion as a bent ditopic acceptor. Two different chelation modes of two ligands around the indium ion were observed in the In–MOM: one was in a *mer*-tridentate/tridentate chelation mode and the other was in a *prop*-bidentate/bidentate chelation mode. A repetition of the two alternating chiral metal ions of different chelation modes leads to the pseudo-D_3-symmetric hexanuclear In–MOM, where the metal ions are in the $\cdots(M_cM_\Delta)(M_cM_\Delta)\cdots$ chiral sequence. Although the formation of the D_3-symmetric In–MOM with smaller ring size is enthalpically unfavorable because of the increased ring strain in the smaller ring system compared with the ring strain of the D_4-symmetric octanuclear Ga–MOM with a larger ring size, the combination of the larger tolerance toward the more distorted coordination geometry of the indium ion having a softer coordination characteristic and a small enthalpy cost for the ligand deformation from the conjugated planar conformation allows the formation of the D_3-symmetric hexanuclear 18-membered In–MOM. While the hexanuclear In–MOM is stable in acetonitrile solution, it partially dissociates into its components in dmso solution, and then slowly reaches a new equilibrium state with at least three different indium complexes yet to be identified in addition to the free ligand. At this moment, we speculate that the new species, **3**, is an S_n-symmetric species based on the triply deprotonated state of the ligand suggested from the ^{1}H NMR spectrum and the relatively slow formation kinetics from the free ligand. We are currently working on the isolation of the new species, **3**.

Acknowledgements

This work was supported by KRF-2008-313-C00424, NRF-2009-0084799, NRF-2010-0019408, and WCU program (R31-2008-000-20012-0). The authors acknowledge PAL for beam line use (2010-3063-10).

Notes and references

1 (*a*) J. R. Long and O. M. Yaghi, *Chem. Soc. Rev.*, 2009, **38**, 1213; (*b*) R. E. Morris and P. S. Wheatley, *Angew. Chem., Int. Ed.*, 2008, **47**, 4966; (*c*) R. Zou, A. I. Abdel-Fattah, H. Xu, Y. Zhao and D. D. Hickmott, *CrystEngComm*, 2010, **12**, 1337; (*d*) J. S. Seo, D. Whang, H. Lee, S. I. Jun, J. Oh, Y. J. Jeon and K. Kim, *Nature*, 2000, **404**, 982; (*e*) P. Horcajada, T. Chalati, C. Serre, B. Gillet, C. Sebrie, T. Baati, J. F. Eubank, D. Heurtaux, P. Clayette, C. Kreuz, J.-S. Chang, Y. K. Hwang, V. Marsaud, P.-N. Bories, L. Cynober, S. Gil, G. Férey, P.

Couvreu and R. Gref, *Nat. Mater.*, 2010, **9**, 172; (*f*) C. B. Aakeröy, N. R. Champness and C. Janiak, *CrystEngComm*, 2010, **12**, 22; (*g*) S. Kitagawa, R. Kitaura and S.-i. Noro, *Angew. Chem., Int. Ed.*, 2004, **43**, 2334; (*h*) M. J. Prakash and M. S. Lah, *Chem. Commun.*, 2009, 3326.

2 (*a*) M. Yoshizawa, J. K. Klosterman and M. Fujita, *Angew. Chem., Int. Ed.*, 2009, **48**, 3418; (*b*) Q.-F. Sun, J. Iwasa, D. Ogawa, Y. Ishido, S. Sato, T. Ozeki, Y. Sei, K. Yamaguchi and M. Fujita, *Science*, 2010, **328**, 1144; (*c*) M. Tominaga, K. Suzuki, M. Kawano, T. Kusukawa, T. Ozeki, S. Sakamoto, K. Yamaguchi and M. Fujita, *Angew. Chem., Int. Ed.*, 2004, **43**, 5621; (*d*) M. D. Pluth, R. G. Bergman and K. N. Raymond, *Science*, 2007, **316**, 85; (*e*) D. L. Caulder, R. E. Powers, T. N. Parac and K. N. Raymond, *Angew. Chem., Int. Ed.*, 1998, **37**, 1840; (*f*) S. R. Seidel and P. J. Stang, *Acc. Chem. Res.*, 2002, **35**, 972; (*g*) H. Furukawa, J. Kim, N. W. Ockwig, M. O'Keeffe and O. M. Yaghi, *J. Am. Chem. Soc.*, 2008, **130**, 11650; (*h*) J. Bai, A. V. Virovets and M. Scheer, *Science*, 2003, **300**, 781; (*i*) D. Moon, S. Kang, J. Park, K. Lee, R. P. John, H. Won, G. H. Seong, Y. S. Kim, G. H. Kim, H. Rhee and M. S. Lah, *J. Am. Chem. Soc.*, 2006, **128**, 3530.

3 (*a*) M. Fujita, M. Tominaga, A. Hori and B. Therrien, *Acc. Chem. Res.*, 2005, **38**, 371; (*b*) B. H. Northrop, Y.-R. Zheng, K.-W. Chi and P. J. Stang, *Acc. Chem. Res.*, 2009, **42**, 1554; (*c*) S. Leininger, B. Olenyuk and P. J. Stang, *Chem. Rev.*, 2000, **100**, 853; (*d*) D. L. Caulder and K. N. Raymond, *J. Chem. Soc., Dalton Trans.*, 1999, 1185; (*e*) G. Mezei, C. M. Zaleski and V. L. Pecoraro, *Chem. Rev.*, 2007, **107**, 4933; (*f*) T. C. Stamatatos, A. G. Christou, C. M. Jones, B. J. O'Callaghan, K. A. Abboud, T. A. O'Brien and G. Christou, *J. Am. Chem. Soc.*, 2007, **129**, 9840; (*g*) C.-Y. Su, Y.-P. Cai, C.-L. Chen, M. D. Smith, W. Kaim and H.-C. zur Loye, *J. Am. Chem. Soc.*, 2003, **125**, 8595; (*h*) X. Song, X. Liu, M. Oh and M. S. Lah, *Dalton Trans.*, 2010, **39**, 6178.

4 (*a*) W. Liu, K. Lee, M. Park, R. P. John, D. Moon, Y. Zou, X. Liu, H.-C. Ri, G. H. Kim and M. S. Lah, *Inorg. Chem.*, 2008, **47**, 8807; (*b*) K. Lee, R. P. John, M. Park, D. Moon, H.-C. Ri, G. H. Kim and M. S. Lah, *Dalton Trans.*, 2008, 131; (*c*) X. Liu, W. Liu, K. Lee, M. Park, H.-C. Ri, G. H. Kim and M. S. Lah, *Dalton Trans.*, 2008, 6579; (*d*) R. P. John, M. Park, D. Moon, K. Lee, S. Hong, Y. Zou, C. S. Hong and M. S. Lah, *J. Am. Chem. Soc.*, 2007, **129**, 14142; (*e*) R. P. John, D. Moon and M. S. Lah, *Supramol. Chem.*, 2007, **19**, 295; (*f*) R. P. John, K. Lee, B. J. Kim, B. J. Suh, H. Rhee and M. S. Lah, *Inorg. Chem.*, 2005, **44**, 7109; (*g*) B. Kwak, H. Rhee and M. S. Lah, *Polyhedron*, 2000, **19**, 1985; (*h*) B. Kwak, H. Rhee, S. Park and M. S. Lah, *Inorg. Chem.*, 1998, **37**, 3599.

5 J. Choi, J. Park, M. Park, D. Moon and M. S. Lah, *Eur. J. Inorg. Chem.*, 2008, 5465.

6 M. Park, R. P. John, D. Moon, K. Lee, G. H. Kim and M. S. Lah, *Dalton Trans.*, 2007, 5412.

7 A. J. Arvai and C. Nielsen, *ADSC Quantum-210 ADX Program*, Area Detector System Corporation, Poway, CA, USA, 1983.

8 Z. Otwinowski and W. Minor, in *Methods in Enzymology*, ed. C. W. Carter Jr. and R. M. Sweet, Academic Press, New York, 1997, 276, part A, p. 307.

9 G. M. Sheldrick, *SHELXTL-Plus, Crystal Structure Analysis Package*, Bruker Analytical X-Ray, Madison, WI, USA, 1997.

10 A. L. Spek, Platon program. (Ver 1.08), *Acta Crystallogr., Sect. A: Found. Crystallogr.*, 1990, **46**, 194.

11 (*a*) M. Schweiger, S. R. Seidel, A. M. Arif and P. J. Stang, *Angew. Chem., Int. Ed.*, 2001, **40**, 3467; (*b*) M. Schweiger, S. R. Seidel, A. M. Arif and P. J. Stang, *Inorg. Chem.*, 2002, **41**, 2556.